OXFORD JOURNAL
OF STUDENT
SCHOLARSHIP

Aerodynamic Impact of Rear-Mounted Delivery Boxes on Motorcycle Drag: Computational Fluid Dynamics Study

Arnav Sumit Lahoti, Nipun Kothare
arnav.lahoti@outlook.com

ABSTRACT

The rise of e-commerce and quick commerce has led to more motorcycles being used for last-mile delivery service with delivery boxes attached to the rear of the bikes. These boxes enhance delivery, but the bluff shape may cause some flow disturbance and increased aerodynamic drag. This study aims to assess the aerodynamic effects of the delivery box geometry on a motorcycle using Computational Fluid Dynamics (CFD) software. Three configurations were examined: the baseline motorcycle, the motorcycle featuring a cubical delivery box and the filleted delivery box motorcycle. ANSYS Fluent was used to simulate the flow at an inlet velocity of 30 km/h, using a steady-state simulation with the Shear Stress Transport (SST) k–ω turbulence model. Streamline visualisations, pressure contours, velocity contours, drag force and drag coefficient were used to compare the configurations.

The results showed that the drag coefficient increased by 65.2% and the drag force by 77.5% when a cubical delivery box was added to the motorcycle compared with the baseline. Compared to the cubical delivery box, the drag force decreased by 22.7%, and the drag coefficient decreased by 23.7%, increasing aerodynamic efficiency for a similar delivery volume. The flow visualisations revealed that the cubical delivery box generated greater flow separation and a larger wake downstream, whereas the filleted geometry produced more uniform flow around the box and a smaller wake. The results indicate that there is a potential aerodynamic benefit in delivery boxes that can be achieved simply through geometric modifications (e.g., filleting the box edges) without compromising their functionality on commercial delivery motorcycles.

Keywords: *Computational Fluid Dynamics; Motorcycle Aerodynamics; Delivery Box Design; Aerodynamic Drag; Wake Formation*

INTRODUCTION

Motivation and Background

Last-mile logistics has been revolutionised globally by the rapid growth of e-commerce and quick-commerce. The expectation that groceries, food, medicine, and other necessities be delivered within minutes, not days, has created demand for fast, cheap, and flexible delivery systems for urban areas (McKinsey, 2018; World Economic Forum, 2020). Because of their low operating costs, high manoeuvrability, and efficient travel on congested city roads, motorcycles and scooters are the backbone of many delivery networks in India. Consequently, two-wheelers have become a vital part of transportation for food delivery, grocery delivery, courier services, pharmacy logistics, and bike taxi services, particularly in urban areas where compact vehicles are ideal for short trips, especially in dense urban areas.

This growth has increased the practical importance of improving delivery-vehicle efficiency. As motorcycles and scooters continue to be used for food delivery, grocery delivery, courier services, pharmacy logistics, and bike taxi services, design features that affect fuel consumption, emissions, and operating cost have become increasingly important.

It is worth emphasising the importance of vehicle efficiency, especially in quick commerce. Delivery motorcycles often operate over short, repeated urban trips from local fulfilment centres. Although the delivery distance is short, riders make many trips throughout the day. As a result, even modest gains in vehicle efficiency can add up to significant savings in fuel and operating costs, as well as in emissions, for a commercial fleet. This is particularly important as the volume of deliveries is projected to grow, and if efficiency-enhancing measures are not implemented, delivery traffic and emissions in urban areas would increase (World Economic Forum, 2020; Goodchild & Toy, 2018; Figliozzi, 2020; International Energy Agency, 2023).

Aerodynamic drag is one of the main factors affecting vehicle efficiency. When a motorcycle is travelling through the air, it encounters a resisting force that is counter to its forward motion. This force depends on vehicle speed, frontal projected area, air density, and drag coefficient. It is a dimensionless measure of aerodynamic efficiency and is commonly used to compare the aerodynamic performances of different vehicle geometries. On conventional motorbikes, a decrease in aerodynamic drag reduces the power required to keep the vehicle moving, resulting in better fuel efficiency (Hoerner, 1965; Hucho, 1998; Anderson, 2017; White, 2016; Barnard, 2009).

Although there have been continuous developments in powertrain technology, relatively little research has focused on the aero performance of commercial delivery motorcycles. Most rear-mounted delivery boxes are designed more with the thought of how much space they can save, how durable they will be, and how easily they can be manufactured, rather than much for aerodynamic resistance. They would expect their shape to alter the airflow around them, increasing the wake behind the motorcycle and increasing the pressure drag. Although these delivery boxes are commonly used in contemporary delivery fleets, only a

handful of quantitative studies have explored their aerodynamic effects using Computational Fluid Dynamics (CFD). The main motivation for this practical engineering problem is the present study.

Previous Research on Motorcycle Aerodynamics

The motorcycle aerodynamics has been studied using experimental and Computational Fluid Dynamics techniques. Motorcycles pose a complex aerodynamic problem, as the rider is an external part of the geometry and there are external wheels, suspension components, handlebars, and engine assemblies that create many flow separation areas. The flow can separate in these zones, creating turbulent wakes behind the motorcycle that increase pressure drag and reduce overall aerodynamic efficiency (Hoerner, 1965; Hucho, 1998; Cossalter, 2006; Katz, 2006).

Numerical and experimental investigations have shown that the aerodynamic efficiency of scooters and motorcycles is highly dependent on the front-end geometry, windshield shape, rider posture, and the vehicle's exposed parts. It has been found that introducing relatively small geometric changes to two-wheelers can change their pressure distribution around the vehicle, as well as their comfort for riders, through wind tunnel tests (Ubertini & Desideri, 2002). CFD studies have also demonstrated that numerical simulation can be used to predict the pressure distributions and aerodynamic drag which are required, with reduced need for repeated tests in a wind tunnel during early design phases of the aircraft (Bella et al., 2003).

However, a few more recent studies have focused on how specific design parameters affect a motorcycle's aerodynamics. Crosswind simulations have demonstrated that yaw angle may influence wake shape, wind gradient, and vehicle stability (Fintelman et al., 2015). Rider posture can also significantly affect aerodynamic performance, and the upright body posture has higher drag coefficient than a low-drag posture in a racing position (Wiński & Piechna, 2022). Likewise, streamlined fairings can help minimise aerodynamic drag by ensuring smoother airflow around the motorcycle. The interaction of the motorcycle rider's geometry creates complex flow structures that significantly affect drag and wake formation, as demonstrated in recent CFD studies of sport motorcycles (Dąbrowski et al., 2022).

The flow around motorcycles exhibits aerodynamic behaviour similar to that of bluff-body flow. A bluff body results in flow separation from the surface, creating a low-pressure wake behind the body. This wake can have a significant impact on pressure drag, particularly if the back shape is sharp or boxy. The Ahmed body is a simple car body model used to investigate the separated wake behavior and the effect of rear geometry on drag and pressure recovery (Ahmed et al., 1984; Hucho, 1998; Choi et al., 2014; Zhang et al., 2021). The same rules apply to delivery boxes, as their cubical shape creates sharp edges and flat back surfaces that can upset the flow behind the rider.

The computational fluid dynamics technique has become an important tool for studying these aerodynamic effects, enabling researchers to visualise pressure contours, velocity fields, streamlines, and wake regions without building multiple physical prototypes. The SST k–ω (k–omega) turbulence model is widely employed in external aerodynamic simulations due to its ability to accurately capture the

behaviour of boundary-layer and separated flows near solid surfaces (Menter, 1994; Pope, 2000; Versteeg & Malalasekera, 2007; ANSYS Inc., 2024). CFD is particularly helpful for student and early-stage design studies, where it can be used to pre-test different geometries.

Research Gap and Objectives

There has been a significant increase in commercial delivery services, leading to millions of motorcycles with delivery boxes mounted on the back. Although common, there have been few studies that quantify the aerodynamic penalty imposed by such delivery boxes or explore whether simple changes to the boxes can improve their aerodynamic performance. The majority of existing motorcycle aerodynamic research has focused on fairings, rider posture and stability, with little attention paid to the aerodynamic properties of delivery motorcycles with boxes mounted on the back.

The present study seeks to fill this void by performing a CFD study of three motorcycle configurations: a baseline motorcycle with no delivery box, a motorcycle with a conventional cubical delivery box, and a motorcycle with a filleted delivery box designed to minimise flow separation. These configurations are then compared for their aerodynamic performance by examining pressure distributions, velocity contours, streamline behaviour, wake development, drag force, and drag coefficient under the same operating conditions. The aims of this research are, therefore, to:

1. Calculate the aerodynamic disadvantage of a standard "cubical" delivery box mounted at the back of a vehicle.
2. Use Computational Fluid Dynamics (CFD) to compare the flow characteristics of a motorcycle with and without a delivery box.
3. Assess the effectiveness of a delivery-box geometry with fillets to disrupt the flow and reduce aerodynamic drag, whilst still maintaining a delivery capacity suitable for practical purposes.

The authors aim to contribute to the development of a more efficient commercial motorcycle by combining Computational Fluid Dynamics with practical application in a delivery vehicle, while demonstrating that relatively simple geometric changes can significantly improve the vehicle's performance without sacrificing functionality.

METHODS

Geometry Development

To isolate the aerodynamic effect of delivery-box geometry, three configurations were selected. The baseline motorcycle without a delivery box was used as a reference case to determine the drag of the motorcycle alone. The cubical delivery box represented a simple conventional storage box with flat faces and sharp edges, which is commonly used because it is easy to manufacture and provides a regular storage volume. The filleted delivery box used the same overall bounding dimensions as the cubical

delivery box but rounded the exposed edges, allowing the study to examine whether a small geometric modification could reduce flow separation while preserving comparable delivery capacity.

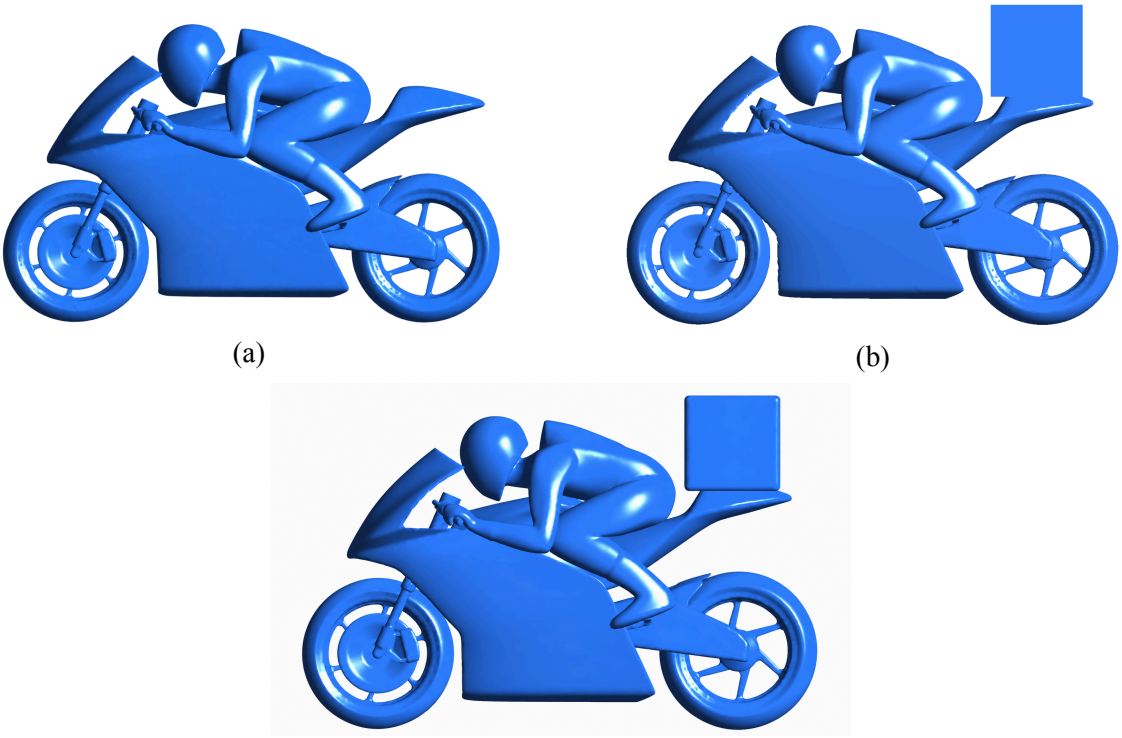

(a) (b)

(c)

Figure 1. Three-dimensional Computer Aided Design (CAD) geometry of the baseline motorcycle with rider and the two delivery-box configurations investigated in this study: (a) baseline motorcycle without delivery box, (b) motorcycle with a rear-mounted cubical delivery box, and (c) motorcycle with a filleted delivery box.

A three-dimensional computer-aided design (CAD) model of a motorcycle was obtained from an open-source library and imported as a STEP (Standard for the Exchange of Product Data) geometry in ANSYS Workbench. The aerodynamic effect of the rear-mounted delivery system was investigated by placing a cubical delivery box, 0.381 m × 0.381 m × 0.381 m (15 in × 15 in × 15 in) directly behind and above the rear seat of the rider. Three basic configurations were studied:

- Case 1: Motorcycle without a delivery box (baseline configuration)
- Case 2: Motorcycle with a rear-mounted cubical delivery box.
- Case 3: Motorcycle with a rear-mounted filleted delivery box.

Figure 1 shows the baseline motorcycle geometry and the two rear-mounted delivery-box configurations used in the study. The cubical and filleted delivery-box models used the same overall bounding

dimensions of 0.381 m × 0.381 m × 0.381 m (15 in × 15 in × 15 in). In the filleted configuration, the overall box envelope was retained while the exposed edges were rounded using a fillet radius of 2 cm. This allowed the two delivery-box designs to preserve comparable delivery volume while isolating the aerodynamic effect of edge rounding.

Computational Domain

The air domain around the motorcycle was created in ANSYS Design Modeler using a cubical shape. The enclosure size was chosen to provide sufficient clearance upstream, downstream, above, and to the sides of the motorcycle, so that the external boundaries do not significantly affect the flow around the motorcycle. The motorcycle volume was subtracted from the enclosure using a Boolean subtraction operation to get the fluid domain for CFD analysis.

Mesh Generation and Convergence

ANSYS Meshing was used to create an unstructured tetrahedral mesh with the Patch Independent algorithm. Small geometric features that were not expected to significantly affect the overall aerodynamic behaviour but would unnecessarily increase mesh density were removed using geometry defeaturing. The final computational mesh for the baseline configuration contained 813,742 elements and 158,609 nodes. A global element size of 1.5 cm, growth rate of 1.2, defeaturing size of 0.02 m, and three inflation layers were used. The inflation layers were applied near the motorcycle and delivery-box wall boundaries to improve near-wall flow resolution and support more reliable prediction of flow separation and wake development.

Mesh quality was assessed using orthogonal quality, with the final mesh achieving a minimum orthogonal quality of 0.73. This indicated that the mesh quality was acceptable for the comparative external-flow CFD simulations. In addition to mesh-quality assessment, a mesh-convergence check was performed for the baseline configuration by testing progressively smaller global element sizes. The predicted baseline drag force decreased as the mesh was refined, and the change became small after the 1.5 cm mesh. Further refinement beyond 1.5 cm changed the predicted drag force by less than 1%, indicating that the selected mesh was sufficiently mesh independent for the comparative CFD analysis.

Based on this convergence behaviour, the 1.5 cm mesh was selected for the final simulations because it provided stable drag results while avoiding unnecessary computational cost. Convergence was also assessed using both scaled residuals and the drag-force monitor. The simulation was considered converged when the scaled residuals decreased below 1×10^{-3} and the monitored drag force showed minimal variation with further iterations. Figure 2 shows the computational domain and final unstructured tetrahedral mesh used for the CFD simulations. The motorcycle geometry was subtracted from the surrounding flow enclosure using a Boolean operation to generate the fluid domain. The inflation layers were used to improve near-wall flow resolution around solid surfaces.

Table 1. Mesh-convergence results for the baseline motorcycle configuration.

Global element size	Baseline drag force	Difference relative to 1.5 cm mesh
10 cm	17.82 N	+4.20%
5 cm	17.66 N	+3.30%
3 cm	17.46 N	+2.11%
1.5 cm	17.10 N	Reference mesh
1.0 cm	17.04 N	−0.37%
0.5 cm	16.94 N	−0.96%

Table 2. Mesh parameters used for the final CFD simulations of the motorcycle configurations

Mesh parameter	Value
Mesh type	Unstructured tetrahedral
Mesh method	Patch Independent
Number of nodes	158,609
Number of elements	813,742
Global element size	0.015 m
Growth rate	1.2
Defeaturing size	0.02 m
Inflation layers	3
Minimum orthogonal quality	0.73

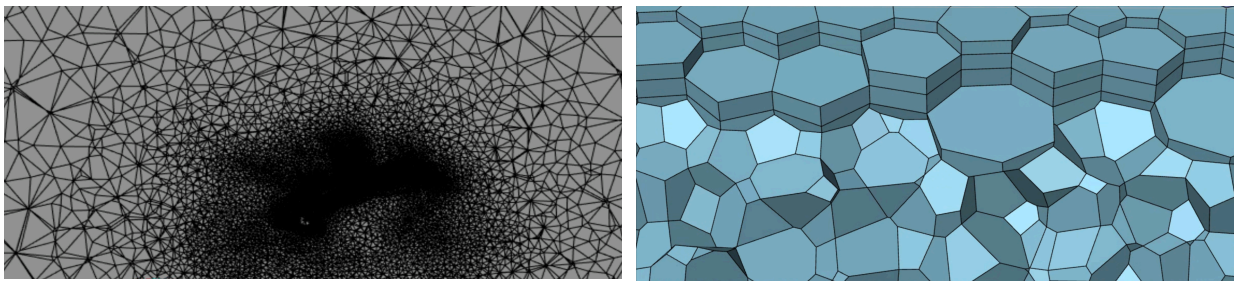

(a) (b)

Figure 2. Computational mesh used for the CFD simulations: (a) computational domain and unstructured tetrahedral mesh around the motorcycle, and (b) close-up view of the inflation-layer mesh near the wall boundary.

Solver Configuration

Simulations were carried out in ANSYS Fluent using a steady-state, pressure-based solver. The flow was modelled as an incompressible Newtonian fluid, and turbulence was modelled using the Shear Stress

Transport (SST) k–ω turbulence model, which is robust for modelling boundary-layer behaviour and flow separation around bluff bodies. A steady state solution of the Navier-Stokes equations was obtained.

Table 3. Solver parameters used in ANSYS Fluent for all three motorcycle configurations, including fluid properties, turbulence model, inlet velocity, outlet condition, wall conditions, initialization method, solution method, and maximum number of iterations.

Parameter	**Value**
Solver Type	Pressure-Based, Steady-State
Working Fluid	Air
Air Density	1.225 kg/m³
Air Viscosity	1.7894×10^{-5} kg/m·s
Turbulence Model	SST k–ω
Inlet Velocity	8.333 m/s (30 km/h)
Outlet Boundary	Pressure Outlet (0 Pa Gauge)
Top & Side Walls	Symmetry
Ground	Moving Wall
Motorcycle Surface	No-Slip Wall
Initialization	Hybrid Initialization
Solution Method	SIMPLE (Semi-Implicit Method for Pressure-Linked Equations)
Maximum Iterations	200

Table 4. Boundary conditions applied to the computational domain for all three motorcycle configurations, including the inlet, outlet, top and side walls, motorcycle surface, and moving ground condition.

Boundary	**Condition**
Inlet	Velocity Inlet (30 km/h or 8.333 m/s)
Outlet	Pressure Outlet (0 Pa gauge pressure)
Top and Side Walls	Symmetry
Motorcycle Surface	No-slip Wall
Ground	Moving wall

The inlet velocity of 30 km/h was selected to represent a typical low-speed urban delivery condition, where motorcycles often operate in congested city traffic rather than at highway speeds. A steady-state simulation was used because the objective of the study was to compare the relative aerodynamic effect of delivery-box geometry under the same controlled operating condition. This approach provides a practical first-stage comparison of drag, pressure distribution, velocity contours, and wake behaviour between the

three configurations. Table 3 summarizes the solver settings used in ANSYS Fluent for all three motorcycle configurations. Table 4 lists the boundary conditions applied to the computational domain for all three motorcycle configurations.

Solution and Post-Processing

The solution was initialised with Hybrid Initialisation and iterated until the scaled residuals decreased below 1×10^{-3} and the monitored drag force showed minimal variation with further iterations. Residual convergence and drag-force stability were used together to confirm that the numerical solution had reached a stable state before post-processing. Figure 3 shows the residual convergence history for the final CFD simulation. The residuals decreased during the iteration process and crossed the 1×10^{-3} convergence threshold before post-processing.

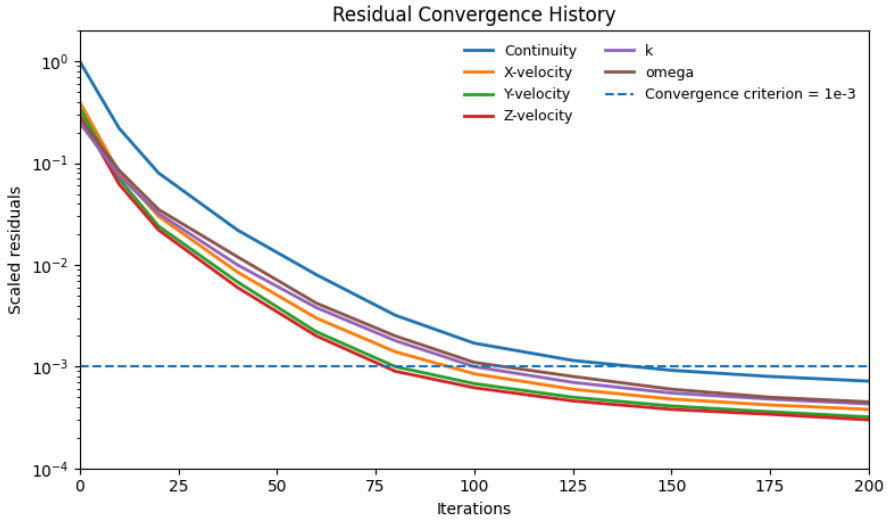

Figure 3. Residual convergence history for the final CFD simulation, plotted on a logarithmic scale. The residuals decreased during the iteration process and crossed the 1×10^{-3} convergence threshold before post-processing.

After convergence, the aerodynamics of each configuration were evaluated using total drag force, drag coefficient, velocity contours, pressure contours, and streamline visualisations. These outputs were selected to represent both quantitative aerodynamic performance and qualitative changes in flow behaviour caused by the rear-mounted delivery box. The results were then compared to understand how delivery-box geometry affected wake formation, pressure distribution, flow separation, and aerodynamic drag.

RESULTS

The flow fields of the baseline motorcycle, the motorcycle with a cubical delivery box, and the motorcycle with a filleted delivery box were compared under the same boundary conditions to investigate the aerodynamic influence of the delivery box geometry. Visualisations of flow, pressure contours, velocity vector plots, and velocity contours were used to qualitatively compare changes in flow attachment, pressure distribution, wake development, and recirculation behaviour. The baseline motorcycle was used as the baseline configuration for the aerodynamic performance of the two delivery-box designs to be compared. Figure 4 compares the streamline visualisations for the baseline motorcycle, cubical delivery-box configuration, and filleted delivery-box configuration.

Region 1 – Front of the Motorcycle

The approach flow to the front of the motorcycle has similar features in all three configurations. A stagnation region is formed in front of the motorcycle at the leading edges, where the air slows before it is turned around the front surfaces of the bike (see Figures 4-6). The delivery box is located downstream of the rider and therefore has little effect on the flow approaching the delivery box, and the pressure and velocity distribution around the front wheel, front fairing, and handlebars are not significantly altered. Local variations can occur as a result of changes in the downstream pressure distribution but these variations are not large enough to affect the aerodynamic behavior of the front of the motorcycle significantly.

Region 2 – Rider and Upper Body

When the air flows over the motorcycle, it speeds up around the rider and helmet, and then separates downstream of the upper body. The flow over the rider's helmet is attached, and then separates, as shown by the streamline patterns in all three configurations, so that the overall flow pattern is more or less the same in all cases. Pressure contours also show similar pressure distributions over the rider, suggesting that the aerodynamic loadings from the rider area are not significantly affected by the presence of the delivery box. Thus the rider will remain the dominant flow field immediately upstream of the delivery box. Figure 5 compares the velocity vector plots for the three motorcycle configurations, showing how the local flow direction and velocity patterns change around the rider and rear delivery-box region.

Region 3 – Rear Delivery Box and Wake Development

The largest aerodynamic differences were observed behind the rider, where the delivery box directly interacted with the separated flow from the motorcycle and rider. In the baseline configuration, the separated air created a relatively compact wake behind the rear seat, which gradually recovered downstream. In contrast, the cubical delivery box introduced a bluff body with sharp edges into this region, causing stronger flow separation and a larger recirculation region behind the vehicle.

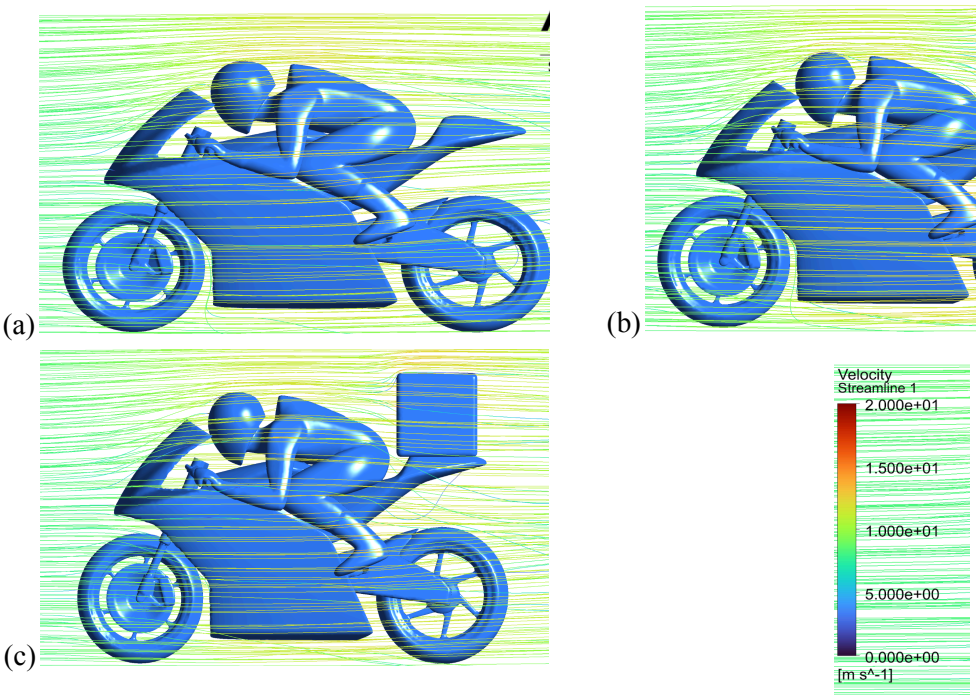

Figure 4. Comparison of streamline visualisations for (a) the baseline motorcycle, (b) the motorcycle with a cubical delivery box, and (c) the motorcycle with a filleted delivery box.

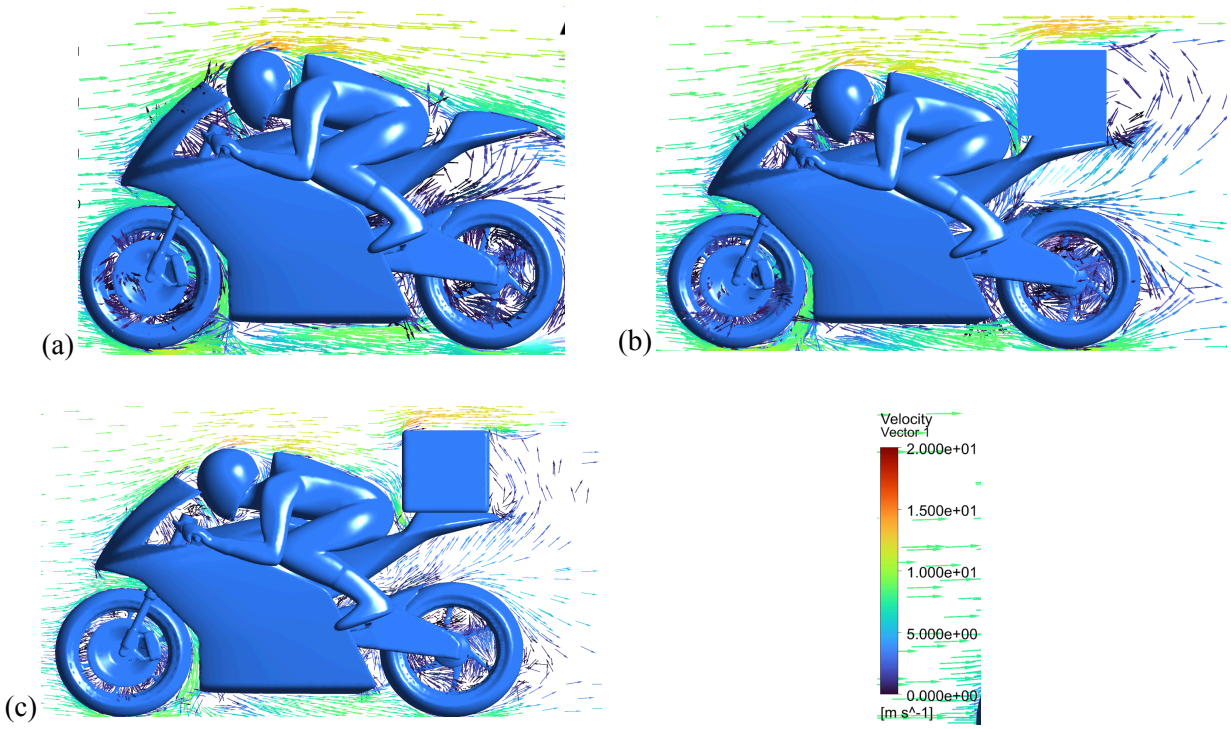

Figure 5. Comparison of velocity vector plots for (a) the baseline motorcycle, (b) the motorcycle with a cubical delivery box, and (c) the motorcycle with a filleted delivery box.

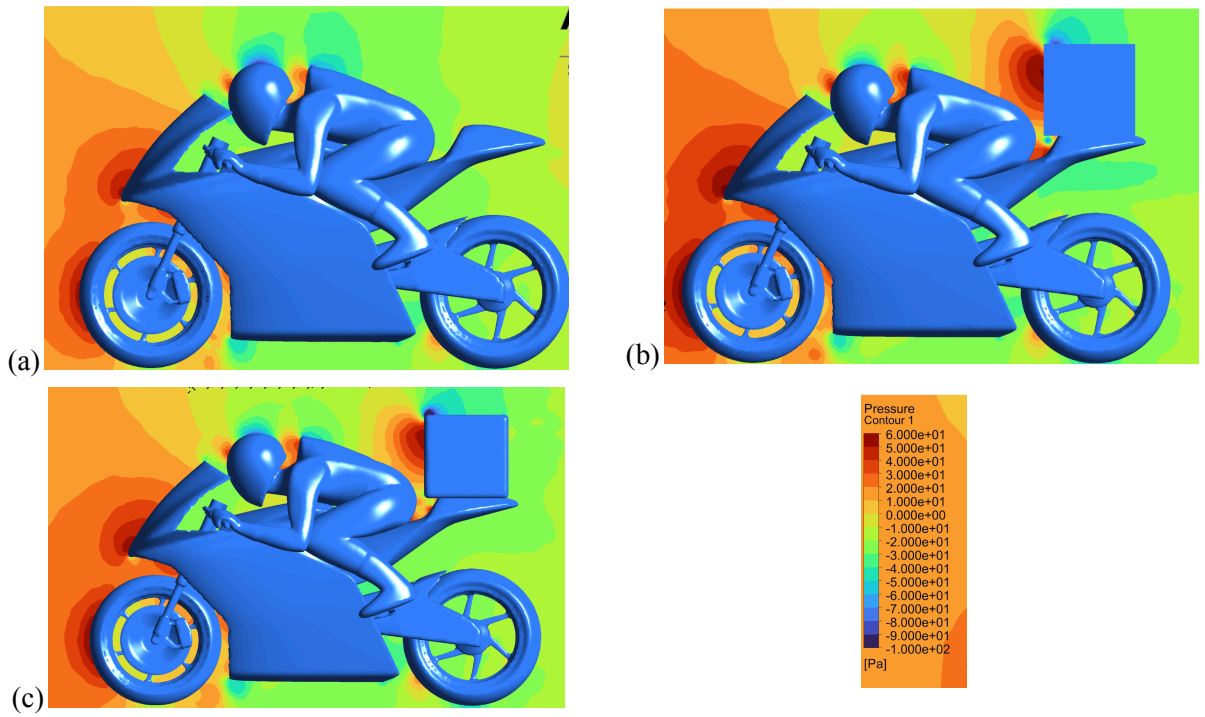

Figure 6. Comparison of pressure contours for (a) the baseline motorcycle, (b) the motorcycle with a cubical delivery box, and (c) the motorcycle with a filleted delivery box.

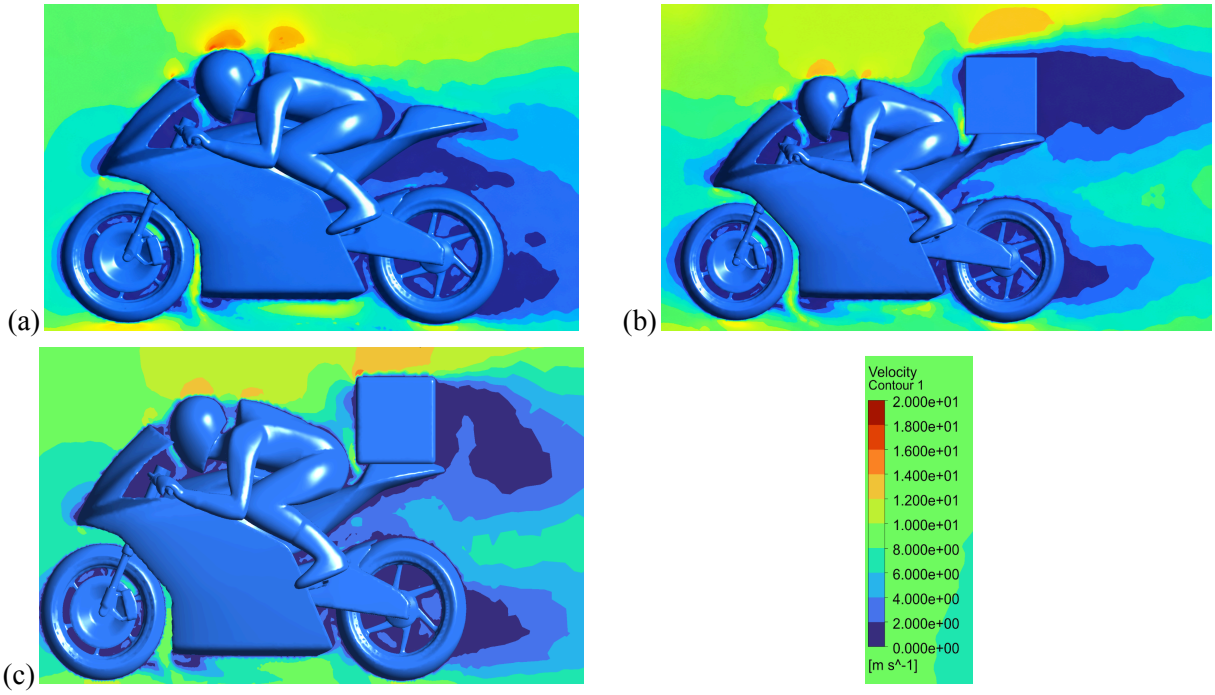

Figure 7. Comparison of velocity contours for (a) the baseline motorcycle, (b) the motorcycle with a cubical delivery box, and (c) the motorcycle with a filleted delivery box.

These pressure contours also show the formation of a distinct high-pressure stagnation zone on the leading face of the delivery box, followed by a long low-pressure wake immediately downstream. This added pressure difference across the delivery box directly increases the pressure drag. The velocity contours also show a larger low-velocity recirculation region trailing the motorcycle and a time delay in velocity recovery compared to the baseline configuration. Together, these findings show that the flow structure downstream of the delivery box is greatly altered and that the aerodynamic resistance measured in the quantitative results is primarily due to the delivery box. Figure 6 compares the pressure contours for the three motorcycle configurations, highlighting the high-pressure region near the front of the delivery box and the low-pressure wake downstream.

Region 4 – Underbody and Rear Wheel

The flow under the motorcycle is only slightly altered with the introduction of the delivery box. The same streamline configurations and velocity distributions occur around the lower frame, swingarm, and rear wheel for the three configurations. A small deviation is observed near the rear wheel due to the modified downstream wake, but it is significantly less than that observed around the delivery box. The underbody, therefore, contributes only a small amount to the total aerodynamic drag. The aerodynamic disadvantage of the delivery box is apparent from the qualitative flow-field comparisons and is associated with increased flow separation, an enlarged wake, and higher pressure drag in the rear part of the motorcycle. A quantitative analysis of these observations is done in the next section, where the drag force and the drag coefficient are compared. Figure 7 compares the velocity contours for the three motorcycle configurations, showing the enlarged low-velocity wake behind the cubical delivery box and the reduced wake region behind the filleted delivery box.

Quantitative Aerodynamic Performance

The aerodynamic results from the previous sections are summarised in Table 5 and provide quantitative support for the qualitative observations. As a reference, the baseline motorcycle was used to assess the aerodynamic effect of the rear-mounted delivery box, with a drag force of 17.1 N and a drag coefficient of 0.69. The projected frontal area of each configuration is also shown to reflect the changes in the effective flow obstruction. Table 5 summarizes the drag force, projected frontal area, and drag coefficient for the three motorcycle configurations.

Table 5. Quantitative aerodynamic performance of the baseline motorcycle, cubical delivery-box configuration, and filleted delivery-box configuration at an inlet velocity of 30 km/h. Percentage changes are calculated relative to the baseline motorcycle.

Configuration	Drag Force F_d (N)	% Change in F_d (wrt to baseline)	Projected Area A (m^2)	Drag Coefficient C_d	% Change in C_d (wrt to baseline)
Baseline Motorcycle	17.1	—	0.58	0.69	—
Cubical Delivery Box	30.4	+77.5%	0.63	1.14	+65.2%
Filleted Delivery Box	23.5	+37.4%	0.63	0.87	+26.1%

The use of conventional cubical delivery boxes added the drag force of 30.4 N (a gain of ~77.5% compared to the baseline motorcycle). The additional drag from the delivery box was also accounted for, resulting in a drag coefficient of 1.14. The results of this study agree with the qualitative flow-field analysis, as the streamline, pressure, and velocity contour visualisations indicate greater flow separation, a larger low-pressure wake, and higher pressure drag behind the motorcycle. Table 6 provides a qualitative summary of wake size and aerodynamic interpretation for the baseline, cubical delivery-box, and filleted delivery-box configurations.

Table 6. Summary of aerodynamic characteristics for the baseline motorcycle, cubical delivery-box configuration, and filleted delivery-box configuration, including drag force, drag coefficient, wake size, and aerodynamic interpretation.

Configuration	Drag Force (N)	Drag Coefficient	Wake Size	Interpretation
Baseline	17.1	0.69	Small	Reference
Cubical Box	30.4	1.14	Large	Highest drag
Filleted Box	23.5	0.87	Moderate	Reduced separation

The filleted geometry reduced the drag of the delivery box to 23.5 N, which is a 22.7% drop from the drag of the cubical delivery box. Smoother leading edges facilitated a more progressive change in the flow direction around the delivery box, thereby minimising flow separation and reducing the size of the downstream recirculation zone. Thus, the drag coefficient also decreased relative to the cubical delivery box, indicating an improvement in aerodynamic efficiency without sacrificing a comparable delivery volume.

The filleted delivery box does not restore the aerodynamic performance of the baseline motorcycle, but it does significantly reduce the aerodynamic penalty of a rear-mounted delivery system. These findings show that the aerodynamic characteristics of the commercial motorcycle delivery can be significantly enhanced by relatively simple geometric changes that do not affect the vehicle's ease of use.

DISCUSSION

From the CFD results, it is evident that the delivery box can significantly influence the bike's aerodynamic performance, particularly at the rear of the vehicle. The motorcycle used as a baseline had the least drag force because there was no large obstruction behind the rider. The wake behind the baseline model was smaller than the delivery box cases, although it did create some flow separation with the motorcycle and rider.

The drag force increased from 17.1 N to 30.4 N when the cubical delivery box was added to the model. This was because the box produced a bluff body directly behind the rider. As the airflow encountered the front face of the cubical delivery box, it formed a high-pressure zone, while the separated flow behind the box created a low-pressure wake. The pressure difference between the front and back of the box was a

significant factor in pressure drag. This is confirmed by the velocity, pressure and streamline plots, which all demonstrate a larger disturbed flow area and delayed flow recovery behind the motorcycle.

The drag force on the delivery box was reduced to 23.5 N after filleting. While the aerodynamics were not the same as those of the original motorcycle, the drag reduction shows significant potential to improve air flow around the delivery box through geometric changes. The rounded leading edges allowed the flow to change direction more gradually, reducing flow separation and decreasing the size of the wake behind the motorcycle.

The decrease in drag may also be attributed to a change in the pressure distribution around the delivery box. The geometry change caused by the sharp corner of the cubical delivery box led to early flow separation and a large low-pressure recirculation region downstream of the motorcycle. The introduction of filleted edges increased the distance the air flowed along the surface before separating. The pressure drag was reduced because the pressure difference between the front and rear faces of the box was reduced by the delayed flow separation. Although flow attachment was not achieved, the delivery box still acts as a bluff body.

These results are also important from an engineering standpoint, as the commercial delivery boxes are required to meet practical criteria in addition to aerodynamic criteria. They must offer adequate storage space, withstand daily use, be easily produced and be compatible with existing motorcycle designs. The idea of completely streamlined delivery boxes would enhance aerodynamic performance, but it would also decrease the box's useful volume and increase its complexity to manufacture. The present study has shown that a relatively simple design modification, such as rounding of the exposed edges while retaining the overall size of the delivery box can result in a significant reduction in aerodynamic drag without sacrificing its intended use. Because the filleted configuration retained the same 0.381 m × 0.381 m × 0.381 m bounding dimensions as the cubical delivery box, the comparison focused on the aerodynamic effect of the 0.02 m edge fillet rather than a change in delivery-box size or storage capacity.

The study also illustrates the applicability of Computational Fluid Dynamics in the design process in the early stages of product development. Although multiple wind tunnel prototypes are not manufactured, various delivery-box designs can be numerically simulated to identify promising designs to build before going to manufacturing. This helps decrease development time and costs, provides a detailed picture of pressure distribution, velocity fields, and streamline behaviour, enables informed engineering decisions, and provides a picture of wake formation.

The present results are based on a single inlet velocity of 30 km/h and a steady-**state** flow assumption. At higher speeds, the absolute drag force would be expected to increase because aerodynamic drag scales with the square of velocity. However, the comparative trend observed in this study, in which the cubical delivery box increases drag and the filleted delivery box reduces part of this penalty, is likely to remain useful for early-stage design screening. Transient simulations and additional inlet speeds could provide a more detailed understanding of unsteady wake behaviour, acceleration effects, and real traffic conditions.

Overall, the study indicated that the main aerodynamic disadvantage is associated with the delivery box rather than the motorcycle itself. The cubical delivery box increases wake size and pressure drag, while the filleted geometry reduces wake size and pressure drag as air flows around the delivery box. Based on these results, the delivery-box geometry needs to be taken into account when designing commercial motorcycles, especially in a growing urban delivery market focused on improving vehicle efficiency.

Limitations

The present study was designed as a controlled comparative CFD investigation supported by numerical verification. Mesh reliability was assessed through mesh refinement, mesh-quality checks, inflation-layer use near wall boundaries, residual convergence, and drag-force monitoring. The final mesh used a 1.5 cm global element size, 813,742 elements, 158,609 nodes, three inflation layers, and a minimum orthogonal quality of 0.73. Further refinement beyond the selected mesh changed the predicted baseline drag force by less than 1%, indicating that the mesh was sufficiently independent for the comparative analysis. In addition, the same computational domain, mesh strategy, turbulence model, inlet velocity, boundary conditions, and post-processing procedure were applied to all three motorcycle configurations. Therefore, the results provide a consistent basis for comparing relative aerodynamic trends between the baseline motorcycle, the cubical delivery-box configuration, and the filleted delivery-box configuration.

The drag values and flow-field visualisations show how delivery-box geometry affects wake formation, pressure distribution, flow separation, and drag under controlled simulation conditions. However, real-world motorcycle airflow may differ from the idealised CFD setup. In actual riding conditions, the motorcycle may experience crosswinds, road-induced turbulence, rider movement, wheel rotation effects, changes in rider posture, and unsteady wake behaviour. These effects were not directly modelled in the present steady-state simulation.

For this reason, the results should be treated as design-level evidence showing the aerodynamic advantage of the filleted delivery-box geometry over the cubical geometry, rather than as exact drag predictions for every real-world operating condition. Future work may include wind-tunnel testing, road testing, transient simulations, crosswind cases, and additional delivery-box geometries to further validate and extend the present findings.

CONCLUSION

In this study, Computational Fluid Dynamics (CFD) was used to determine the aerodynamic effects of rear-mounted delivery boxes on motorcycles. Three configurations were examined: a baseline motorcycle, a motorcycle fitted with a cubical delivery box, and a motorcycle fitted with a filleted delivery box. They were analysed using streamline visualisation, pressure contour plots, velocity contour plots, drag force, and drag coefficient.

The results indicated that aerodynamic drag was increased by the cubical delivery box, which increased the wake region and increased the pressure drag after the motorcycle. This aerodynamic cost was reduced

by introducing filleted edges, which improved flow around the delivery box, reduced flow separation, and minimised the size of the downstream wake. The filleted shape did not restore the aerodynamic performance of the baseline motorcycle. However, it improved the motorcycle's aerodynamic properties compared with the cubical shape while still serving the practical purpose of a delivery box.

The results of the CFD analysis are used to compare the aerodynamic behaviour of the three delivery box configurations under the same simulation conditions. In general, the results indicate that very basic geometric changes can enhance the aerodynamics of a commercial delivery motorcycle and, as a consequence, improve its aerodynamic efficiency without giving up payload capacity. The study also shows that CFD can be an effective design tool for evaluating and optimising delivery-box geometries before physical prototyping. Further research should evaluate transient flow conditions, crosswind effects, rider movement, wheel rotation, different delivery-box dimensions, alternative mounting positions, and experimental validation through wind-tunnel or road testing to further assess the aerodynamic performance of delivery motorcycles under real-world operating conditions.

REFERENCES

1. McKinsey & Company. (2018). *Fast forwarding last-mile delivery: Implications for the ecosystem*. McKinsey & Company.
2. World Economic Forum. (2020). *The future of the last-mile ecosystem*. World Economic Forum.
3. Goodchild, A., & Toy, J. (2018). Delivery by drone: An evaluation of unmanned aerial vehicle technology in reducing CO_2 emissions in the delivery service industry. *Transportation Research Part D: Transport and Environment, 61*, 58–67.
4. Figliozzi, M. A. (2020). Carbon emissions reductions in the last mile and grocery deliveries utilizing air and ground autonomous vehicles. *Transportation Research Part D: Transport and Environment, 85*, 102443.
5. International Energy Agency. (2023). *Road transport*. International Energy Agency.
6. Hoerner, S. F. (1965). *Fluid-dynamic drag*. Hoerner Fluid Dynamics.
7. Hucho, W.-H. (1998). *Aerodynamics of road vehicles* (4th ed.). SAE International.
8. Anderson, J. D. (2017). *Fundamentals of aerodynamics* (6th ed.). McGraw-Hill Education.
9. White, F. M. (2016). *Fluid mechanics* (8th ed.). McGraw-Hill Education.
10. Barnard, R. H. (2009). *Road vehicle aerodynamic design: An introduction* (3rd ed.). MechAero Publishing.
11. Cossalter, V. (2006). *Motorcycle dynamics* (2nd ed.). Lulu.
12. Katz, J. (2006). *Race car aerodynamics: Designing for speed*. Bentley Publishers.
13. Ubertini, S., & Desideri, U. (2002). Aerodynamic investigation of a scooter by numerical and experimental techniques. *SAE Technical Paper 2002-01-1315*. https://doi.org/10.4271/2002-01-1315
14. Bella, G., Biancolini, M. E., & Brutti, C. (2003). Experimental and computational analysis of the aerodynamic performances of a maxi-scooter. *SAE Technical Paper 2003-32-0038*. https://doi.org/10.4271/2003-32-0038

15. Fintelman, D. M., Hemida, H., Sterling, M., & Li, F.-X. (2015). CFD simulations of the flow around a motorcycle subjected to crosswinds. *Journal of Wind Engineering and Industrial Aerodynamics, 144*, 31–41.
16. Wiński, M., & Piechna, J. (2022). Numerical investigation of the influence of rider position on motorcycle aerodynamic performance. *Energies, 15*(18), 6814.
17. Dąbrowski, D., Ślaski, G., Maciejewski, M., & Waluś, K. J. (2022). Comprehensive CFD aerodynamic simulation of a sport motorcycle. *Energies, 15*(16), 5920.
18. Ahmed, S. R., Ramm, G., & Faltin, G. (1984). Some salient features of the time-averaged ground vehicle wake. *SAE Technical Paper 840300*. https://doi.org/10.4271/840300
19. Choi, H., Lee, J., & Park, H. (2014). Aerodynamics of heavy vehicles. *Annual Review of Fluid Mechanics, 46*, 441–468.
20. Zhang, Y., Li, X., & Wang, H. (2021). Numerical investigation of bluff-body wake characteristics and drag reduction strategies using computational fluid dynamics. *Applied Sciences, 11*(9), 4128.
21. Menter, F. R. (1994). Two-equation eddy-viscosity turbulence models for engineering applications. *AIAA Journal, 32*(8), 1598–1605.
22. Pope, S. B. (2000). *Turbulent flows*. Cambridge University Press.
23. Versteeg, H. K., & Malalasekera, W. (2007). *An introduction to computational fluid dynamics: The finite volume method* (2nd ed.). Pearson Education.
24. ANSYS Inc. (2024). *ANSYS Fluent theory guide*. ANSYS, Inc.